Two-phase nozzle flow and the subcharacteristic condition

Gaute Linga[a], Peder Aursand[a,b], Tore Flåtten[c,*]

[a] *SINTEF Energy Research, P. O. Box 4761 Sluppen, NO-7465 Trondheim, Norway*
[b] *Dept. of Mathematical Sciences, Norwegian University of Science and Technology (NTNU), NO-7491 Trondheim, Norway*
[c] *SINTEF Materials and Chemistry, P. O. Box 4760 Sluppen, NO-7465 Trondheim, Norway*

Abstract

We consider nozzle flow models for two-phase flow with phase transfer. Such models are based on energy considerations applied to the frozen and equilibrium limits of the underlying relaxation models.

In this paper, we provide an explicit link between the mass flow rate predicted by these models and the classical *subcharacteristic condition* of Chen–Levermore–Liu. In particular, we demonstrate that for sufficiently small pressure differences, the equilibrium nozzle model will predict a lower mass flow rate than the frozen model when the subcharacteristic condition is satisfied.

An application to tank leakage of CO_2 is presented, indicating that the frozen and equilibrium models provide significantly different predictions. This difference is comparable in magnitude to the modeling error introduced by applying simple ideal-gas/incompressible-liquid equations-of-state for CO_2.

Keywords: Nozzle flow, two-phase flow, subcharacteristic condition
2000 MSC: 76T10, 35L65

---

*Corresponding author.
Email addresses: `gaute.linga@sintef.no` (Gaute Linga), `peder.aursand@math.ntnu.no` (Peder Aursand), `Tore.Flatten@sintef.no` (Tore Flåtten)

1. Introduction

We are interested in mathematical models for two-phase *nozzle flow*, i.e. flow through an orifice driven by pressure differences between the inlet and outlet conditions [29]. Such flows are relevant in numerous applications, such as rocket engine nozzles [28], emergency systems for nuclear power plants [1], as well as valves and cracks in pipeline systems [2, 13]. Due to the curved streamlines involved in such flows, one-dimensional averaged models [17, 22] need to take non-conservative geometry terms into account [4, 12] and solving the full three-dimensional flow models can be too cumbersome.

Instead, the unknown flow variables may be obtained from *energy invariants* transported along the streamlines. This approach, analogous to the Hamiltonian methods of classical mechanics, generalizes the Bernoulli principle from incompressible flows and has proved highly useful for simplified modeling of such complex flow phenomena [21, 24].

In this paper, we are concerned with the nozzle flow theory for a two-phase flow model involving phase transfer. This model, investigated in detail in [3, 5, 7, 10, 13, 16, 25], may be written as a *hyperbolic relaxation system* as follows:

$$\partial_t(\alpha_{\mathrm{g}}\rho_{\mathrm{g}}) + \nabla\cdot(\alpha_{\mathrm{g}}\rho_{\mathrm{g}}\boldsymbol{u}) = \frac{1}{\varepsilon}(\mu_\ell - \mu_{\mathrm{g}}), \tag{1a}$$

$$\partial_t(\alpha_\ell\rho_\ell) + \nabla\cdot(\alpha_\ell\rho_\ell\boldsymbol{u}) = \frac{1}{\varepsilon}(\mu_{\mathrm{g}} - \mu_\ell), \tag{1b}$$

$$\partial_t(\rho u_j) + \sum_{k=1}^{3}\partial_{x_k}(\rho u_j u_k) + \partial_{x_j} p = 0, \tag{1c}$$

$$\partial_t E + \nabla\cdot(\boldsymbol{u}(E+p)) = 0. \tag{1d}$$

Herein, the parameter ε is some characteristic relaxation time, and the indices g and ℓ represent the gas and liquid phase, respectively. The volume fractions α_i of phase i satisfy the relation

$$\alpha_{\mathrm{g}} + \alpha_\ell = 1. \tag{2}$$

Furthermore, ρ_i is the density, and $\boldsymbol{u}$ is the common velocity vector. For each phase $i \in \{\mathrm{g}, \ell\}$, the common pressure p satisfies a separate state relation

$$p = p_i(\rho_i, e_i), \tag{3}$$

where e_i is the specific internal energy. In addition, E is the total energy of the mixture, given by

$$E = \alpha_{\mathrm{g}}\rho_{\mathrm{g}}e_{\mathrm{g}} + \alpha_\ell\rho_\ell e_\ell + \tfrac{1}{2}\rho|\boldsymbol{u}|^2, \tag{4}$$

where

$$\rho = \alpha_{\mathrm{g}}\rho_{\mathrm{g}} + \alpha_\ell\rho_\ell \tag{5}$$

is the mixture density. Finally, μ_i is the chemical potential given by

$$\mu_i = e_i + \frac{p}{\rho_i} - Ts_i, \tag{6}$$

where T is the common temperature and s_i is the specific entropy of phase i.

1.1. Outline

In this paper we provide a direct link between the established nozzle flow theory [13] for the model (1a)–(1d) and the classical *subcharacteristic condition* of Chen–Levermore–Liu [6]. More precisely, we establish that if the flow is driven by a sufficiently small pressure difference, the equilibrium mass flow rate will be lower than the frozen flow rate when the relaxation model (1a)–(1d) satisfies the subcharacteristic condition.

This observation is well known in the engineering community [2, 11]. The purpose of this paper is to emphasize the fundamental *mathematical* relationships underlying this observation, and in particular we provide a connection between *energy* principles and *stability* principles that to the best of our knowledge has so far never been made explicit. The subcharacteristic condition is necessary and sufficient for linear stability [26], and it holds for our current model subject only to fundamental thermodynamic stability conditions [7].

In this respect, our paper builds heavily on the previous works [7, 8, 13]. We explicitly show how the subcharacteristic condition, as verified in [7], provides a mathematical relationship between the flow rates derived in [13].

Our paper is organized as follows. In Section 2, we present some established theory for general hyperbolic relaxation systems and define the crucial concept of the *subcharacteristic condition*. In Section 3, we derive the energy invariants associated with the frozen and equilibrium limits of the model (1a)–(1d). In Section 4, we derive some useful differentials and demonstrate that our models satisfy the subcharacteristic condition. In Section 5, we describe the nozzle flow theory associated with these invariants. In this respect, we consider the theoretical results derived in [13] in the context of general thermodynamic state equations. In particular, we present explicit expressions for the predicted mass flow rates and present the essential result of our paper; the relationship between the flow rates and the subcharacteristic condition.

In Section 6, we present an application of this theory to the simulation of tank leakage of CO_2. We describe a highly simplified model for phase transitions, obtained by combining the incompressible and ideal-gas limits of the stiffened gas equation-of-state [9, 18, 19]. We demonstrate a significant difference between the equilibrium and frozen nozzle flow models in terms of the dynamic development of the tank pressure. We also simulate this problem using a highly accurate equation-of-state for equilibrium CO_2. Our simulations indicate that the difference between the predictions of the equilibrium and frozen nozzle models is in the order of magnitude as the error introduced by employing the highly simplified thermodynamic model.

The main conclusions to be drawn from our paper are summarized in Section 7.

2. Hyperbolic relaxation systems

A general hyperbolic relaxation system in D space dimensions can be written in the form [6]

$$\partial_t \boldsymbol{U} + \nabla \cdot \boldsymbol{F}(\boldsymbol{U}) = \frac{1}{\varepsilon}\boldsymbol{Q}(\boldsymbol{U}), \tag{7}$$

where $\boldsymbol{U} \in G \subseteq \mathbb{R}^N$ is the vector of N unknown variables, $\boldsymbol{F}$ is the vector of fluxes, and $\boldsymbol{Q}$ is a source term acting to drive the system towards the equilibrium state characterized by

$$\boldsymbol{Q}(\boldsymbol{U}) = 0. \tag{8}$$

Herein, ε can be interpreted as a characteristic relaxation time and we assume that the matrix $\boldsymbol{A} = \nabla_{\boldsymbol{U}} \boldsymbol{F} \cdot \boldsymbol{\xi}$ is diagonalizable with real eigenvalues for every wave number $\boldsymbol{\xi} \in \mathbb{R}^D$.

The limit cases corresponding to $\varepsilon \to 0$ and $\varepsilon \to \infty$ will form the main focus of the investigations of this paper. Following [26], we make the following definitions:

- The *non-stiff limit* is characterized by $\varepsilon \to \infty$. In this limit, we may write (7) as
$$\partial_t \boldsymbol{U} + \nabla \cdot \boldsymbol{F}(\boldsymbol{U}) = 0. \tag{9}$$
We will denote (9) as the *frozen system*.

- The formal *equilibrium limit* is characterized by $\boldsymbol{Q}(\boldsymbol{U}) \equiv 0$. This assumption defines an equilibrium manifold [6] through
$$M = \{\boldsymbol{U} \in G : \boldsymbol{Q}(\boldsymbol{U}) = 0\}. \tag{10}$$
Imposing local equilibrium, we may express (7) as
$$\partial_t \hat{\boldsymbol{U}} + \nabla \cdot \hat{\boldsymbol{F}}(\hat{\boldsymbol{U}}) = 0, \tag{11}$$
for some reduced variable $\hat{\boldsymbol{U}}(x,t) \in \mathbb{R}^n$, where $n \leq N$. Herein, every $\hat{\boldsymbol{U}}$ uniquely defines an equilibrium state $\mathcal{E}(\hat{\boldsymbol{U}}) \in M$.

  We will denote (11) as the *equilibrium system*.

2.1. The subcharacteristic condition

Central to our investigations is the concept of the *subcharacteristic condition* [14, 30], first introduced by Leray and subsequently independently found by Whitham. The modern terminology was introduced by Liu [15] for nonlinear 2×2 systems.

For general $N \times N$ hyperbolic relaxation systems in D space dimensions, the condition may be stated as follows [6].

Definition 1. Consider a wave number $\boldsymbol{\xi} \in \mathbb{R}^D$. Let the N eigenvalues of the homogeneous system (9) be given by
$$\lambda_1 \leq \cdots \leq \lambda_k \leq \lambda_{k+1} \leq \cdots \leq \lambda_N, \tag{12}$$
i.e. λ_k are the eigenvalues of
$$\boldsymbol{A} = \frac{\partial \boldsymbol{F}}{\partial \boldsymbol{U}} \cdot \boldsymbol{\xi}. \tag{13}$$
Let $\hat{\lambda}_j$ be the n eigenvalues of the equilibrium system (11), i.e. $\hat{\lambda}_j$ are the eigenvalues of
$$\boldsymbol{B} = \frac{\partial \hat{\boldsymbol{F}}}{\partial \hat{\boldsymbol{U}}} \cdot \boldsymbol{\xi}. \tag{14}$$

Herein, the homogeneous system (9) is applied to a local equilibrium state $\boldsymbol{U} = \mathcal{E}(\hat{\boldsymbol{U}})$, such that

$$\lambda_k = \lambda_k(\mathcal{E}(\hat{\boldsymbol{U}})), \qquad \hat{\lambda}_j = \hat{\lambda}_j(\hat{\boldsymbol{U}}). \tag{15}$$

The equilibrium system (11) is said to satisfy the **subcharacteristic condition** with respect to (9) when the following statements hold:

1. all $\hat{\lambda}_j$ are real;
2. if the $\hat{\lambda}_j$ are sorted in ascending order as

$$\hat{\lambda}_1 \leq \cdots \leq \hat{\lambda}_j \leq \hat{\lambda}_{j+1} \leq \cdots \leq \hat{\lambda}_n, \tag{16}$$

   then $\hat{\lambda}_j$ are interlaced with $\hat{\lambda}_k$ in the following sense: Each $\hat{\lambda}_j$ lies in the closed interval $[\lambda_j, \lambda_{j+N-m}]$.

2.2. Stability

Chen et al. [6] introduced an entropy condition which they proved implies the subcharacteristic condition. Yong [31] proved that for relaxation systems satisfying $n = N-1$, the subcharacteristic condition is necessary for the linear stability of the equilibrium state. An explicit proof that it is also sufficient was stated in [26]. Hence for rank 1 relaxation systems the subcharacteristic condition is precisely the linear stability condition.

3. Energy invariants

Observing that the model (1a)–(1d) is a rank 1 relaxation system as described in Section 2, we now turn to deriving energy invariants for the frozen and equilibrium limits of this model.

In particular, we are interested in quantities that remain constant along streamlines for stationary flows. Noting that streamlines are everywhere tangent to the local velocity field, we may state the following definition.

Definition 2. Assume that a flow parameter B is constant along streamlines for steady flows such that

$$\boldsymbol{u} \cdot \nabla \boldsymbol{B} = 0. \tag{17}$$

Then B is denoted a streamline invariant.

In the present context, this definition is related to the conservation of scalar quantities as follows.

Proposition 1. Assume that we for some variable ξ have the conservation equation

$$\partial_t \xi + \nabla \cdot (\rho B \boldsymbol{u}) = 0. \tag{18}$$

Then B is a streamline invariant for steady flows.

Proof. By adding (1a) to (1b) we observe that for steady flows we have

$$\nabla \cdot (\rho \boldsymbol{u}) = 0. \tag{19}$$

Furthermore,

$$\nabla \cdot (\rho B \boldsymbol{u}) = \rho \boldsymbol{u} \cdot \nabla B + B \nabla \cdot (\rho \boldsymbol{u}) = \rho \boldsymbol{u} \cdot \nabla B, \tag{20}$$

and we recover (17) by dividing by ρ. □

3.1. The equilibrium limit

In the equilibrium limit, we recover the classical *homogeneous equilibrium model* given by

$$\partial_t \rho + \nabla \cdot (\rho \boldsymbol{u}) = 0, \tag{21a}$$

$$\partial_t (\rho u_j) + \sum_{k=1}^{3} \partial_{x_k} (\rho u_j u_k) + \partial_{x_j} p = 0, \tag{21b}$$

$$\partial_t E + \nabla \cdot (\boldsymbol{u}(E + p)) = 0, \tag{21c}$$

supplemented with the closure relations

$$\mu_{\mathrm{g}} = \mu_\ell = \mu, \tag{22}$$

$$p_{\mathrm{g}} = p_\ell = p, \tag{23}$$

$$T_{\mathrm{g}} = T_\ell = T. \tag{24}$$

Note that this is precisely the Euler model expressed in mixture variables. We now define the mixture specific energy, enthalpy and entropy as follows:

$$e = \frac{\alpha_{\mathrm{g}} \rho_{\mathrm{g}} e_{\mathrm{g}} + \alpha_\ell \rho_\ell e_\ell}{\rho}, \tag{25}$$

$$h = e + \frac{p}{\rho}, \tag{26}$$

$$s = \frac{\alpha_{\mathrm{g}} \rho_{\mathrm{g}} s_{\mathrm{g}} + \alpha_\ell \rho_\ell s_\ell}{\rho}. \tag{27}$$

We then have the following observations.

Proposition 2. The mixture *stagnation* enthalpy

$$h_{\mathrm{s}} = h + \tfrac{1}{2}|\boldsymbol{u}|^2 \tag{28}$$

is a streamline invariant for the equilibrium model.

Proof. The result follows from (21c), Proposition 1 and the relation

$$E + p = \rho\left(h + \tfrac{1}{2}|\boldsymbol{u}|^2\right). \tag{29}$$

□

Proposition 3. The mixture entropy s is a streamline invariant for the equilibrium model.

Proof. This is a classical result from fluid mechanics, but we state the proof for completeness. The fundamental thermodynamic differential expressed in the mixture variables is

$$\mathrm{d}e = T\,\mathrm{d}s + \frac{p}{\rho^2}\,\mathrm{d}\rho. \tag{30}$$

Furthermore, from (21a) and (21b) we have

$$\frac{p}{\rho}\partial_t\rho + \partial_t\left(\tfrac{1}{2}\rho|\boldsymbol{u}|^2\right) + \frac{p}{\rho}\boldsymbol{u}\cdot\nabla\rho + \nabla\cdot\left(\boldsymbol{u}\left(\tfrac{1}{2}\rho|\boldsymbol{u}|^2 + p\right)\right) = 0, \tag{31}$$

which by (21a) and (30) can be written as

$$\begin{aligned}\partial_t(\rho e) - \rho T\partial_t s + \partial_t\left(\tfrac{1}{2}\rho|\boldsymbol{u}|^2\right)& \\ + \nabla\cdot(\rho e\boldsymbol{u}) - \rho T\boldsymbol{u}\cdot\nabla s + \nabla\cdot\left(\boldsymbol{u}\left(\tfrac{1}{2}\rho|\boldsymbol{u}|^2 + p\right)\right) &= 0.\end{aligned} \tag{32}$$

Comparing this with (21c) yields

$$\partial_t s + \boldsymbol{u}\cdot\nabla s = 0. \tag{33}$$

□

3.2. The frozen limit

We now turn to the frozen limit of the model, i.e. the model given by

$$\partial_t(\alpha_{\mathrm{g}}\rho_{\mathrm{g}}) + \nabla\cdot(\alpha_{\mathrm{g}}\rho_{\mathrm{g}}\boldsymbol{u}) = 0, \tag{34a}$$

$$\partial_t(\alpha_\ell\rho_\ell) + \nabla\cdot(\alpha_\ell\rho_\ell\boldsymbol{u}) = 0, \tag{34b}$$

$$\partial_t(\rho u_j) + \sum_{k=1}^{3}\partial_{x_k}(\rho u_j u_k) + \partial_{x_j}p = 0, \tag{34c}$$

$$\partial_t E + \nabla\cdot(\boldsymbol{u}(E+p)) = 0. \tag{34d}$$

Proposition 4. The mass fraction

$$Y = \frac{\alpha_{\mathrm{g}} \rho_{\mathrm{g}}}{\rho} \tag{35}$$

is a streamline invariant for the frozen model.

Proof. We may write (34a) as

$$\partial_t(\rho Y) + \nabla \cdot (\rho Y \boldsymbol{u}) = 0. \tag{36}$$

The result now follows from Proposition 1. □

Proposition 5. The mixture stagnation enthalpy

$$h_{\mathrm{s}} = h + \tfrac{1}{2}|\boldsymbol{u}|^2 \tag{37}$$

is a streamline invariant for the frozen model.

Proof. The proof is the same as for Proposition 2. □

Proposition 6. The mixture entropy s is a streamline invariant for the frozen model.

Proof. For this system, the fundamental thermodynamic differential becomes

$$\mathrm{d}e = T\,\mathrm{d}s + \frac{p}{\rho^2}\,\mathrm{d}\rho + (\mu_{\mathrm{g}} - \mu_\ell)\,\mathrm{d}Y. \tag{38}$$

By the mass equations (34a)–(34b), we may write (38) as

$$\partial_t(\rho e) + \nabla \cdot (\rho e \boldsymbol{u}) = \rho T \partial_t s + \rho T \boldsymbol{u} \cdot \nabla s - p \nabla \cdot \boldsymbol{u}. \tag{39}$$

From (34a)–(34c) we may derive the kinetic energy evolution equation

$$\partial_t \left(\tfrac{1}{2}\rho|\boldsymbol{u}|^2\right) + \nabla \cdot \left(\boldsymbol{u}\left(\tfrac{1}{2}\rho|\boldsymbol{u}|^2\right)\right) + \boldsymbol{u} \cdot \nabla p = 0. \tag{40}$$

Now using (34d) and (40) we obtain

$$\partial_t s + \boldsymbol{u} \cdot \nabla s = 0. \tag{41}$$

□

4. Sound velocities

Having established some mathematical properties of these models, we now revisit the *subcharacteristic condition*. Given that this condition is equivalent to the linear stability of the relaxation process [26], it is expected to hold for the frozen and equilibrium flow models considered in this paper.

An explicit calculation verifying this condition was given in [7] for the one-dimensional versions of the models. Due to the space symmetry, the result carries over also to our full three-dimensional models. In particular, for our models the subcharacteristic condition in the sense of Definition 1 reduces to [7]

$$\hat{c} \leq \tilde{c}, \tag{42}$$

where $\hat{c}$ is the sound velocity of the equilibrium model and $\tilde{c}$ is the sound velocity of the frozen model. In particular, we have [7]:

$$\tilde{c}^{-2} = \left(\frac{\partial \rho}{\partial p}\right)_{Y,s} = \rho\left(\frac{\alpha_{\mathrm{g}}}{\rho_{\mathrm{g}} c_{\mathrm{g}}^2} + \frac{\alpha_\ell}{\rho_\ell c_\ell^2} + \frac{C_{p,\mathrm{g}} C_{p,\ell}(\zeta_\ell - \zeta_{\mathrm{g}})^2}{T(C_{p,\mathrm{g}} + C_{p,\ell})}\right), \tag{43}$$

$$\hat{c}^{-2} = \rho\left(\frac{\alpha_{\mathrm{g}}}{\rho_{\mathrm{g}} c_{\mathrm{g}}^2} + \frac{\alpha_\ell}{\rho_\ell c_\ell^2} + T\left(C_{p,\mathrm{g}}\left(\frac{\zeta_{\mathrm{g}}}{T} + W\right)^2 + C_{p,\ell}\left(\frac{\zeta_\ell}{T} + W\right)^2\right)\right), \tag{44}$$

where

$$c_i^2 = \left(\frac{\partial p}{\partial \rho}\right)_s, \tag{45}$$

$$C_{p,i} = \rho_i \alpha_i T \left(\frac{\partial s_i}{\partial T}\right)_p, \tag{46}$$

$$\zeta_i = \left(\frac{\partial T}{\partial p}\right)_{s_i}, \tag{47}$$

$$W = \frac{1}{\rho_{\mathrm{g}}\rho_\ell} \frac{\rho_{\mathrm{g}} - \rho_\ell}{h_{\mathrm{g}} - h_\ell}. \tag{48}$$

4.1. The subcharacteristic condition

From [25] we have the differential

$$\mathrm{d}(\mu_{\mathrm{g}} - \mu_\ell) = \left(\beta\frac{\rho\tilde{c}^2}{\rho_{\mathrm{g}}} - h_{\mathrm{g}}\mathcal{M}_\epsilon\right)\mathrm{d}(\rho_{\mathrm{g}}\alpha_{\mathrm{g}}) + \left(\beta\frac{\rho\tilde{c}^2}{\rho_\ell} - h_\ell\mathcal{M}_\epsilon\right)\mathrm{d}(\rho_\ell\alpha_\ell) + \mathcal{M}_\epsilon\,\mathrm{d}(\rho e), \tag{49}$$

where

$$\Theta = \frac{\zeta_{\rm g} C_{p,{\rm g}} + \zeta_\ell C_{p,\ell}}{C_{p,{\rm g}} + C_{p,\ell}}, \tag{50}$$

$$\beta = \frac{1}{\rho_{\rm g}} - \frac{1}{\rho_\ell} + \Theta(s_\ell - s_{\rm g}), \tag{51}$$

$$\mathcal{M}_\epsilon = \mathcal{P}_\epsilon \beta + \frac{s_\ell - s_{\rm g}}{C_{p,{\rm g}} + C_{p,\ell}}. \tag{52}$$

We may now write (49) as

$$\mathrm{d}(\mu_{\rm g} - \mu_\ell) = \left(\beta \frac{\rho \tilde{c}^2}{\rho_{\rm g}} - h_{\rm g} \mathcal{M}_\epsilon\right) \mathrm{d}(\rho Y) + \left(\beta \frac{\rho \tilde{c}^2}{\rho_\ell} - h_\ell \mathcal{M}_\epsilon\right) \mathrm{d}(\rho(1 - Y)) + \rho \mathcal{M}_\epsilon \,\mathrm{d}e + e \mathcal{M}_\epsilon \,\mathrm{d}\rho = 0. \tag{53}$$

Introducing the shorthand

$$\nu = \rho T \frac{(s_\ell - s_{\rm g})^2}{C_{p,{\rm g}} + C_{p,\ell}} \tag{54}$$

and using (38), we may rewrite (53) as

$$\beta \tilde{c}^2 \,\mathrm{d}\rho + \left(\beta^2 \rho^2 \tilde{c}^2 + \nu\right) \mathrm{d}Y + \rho \mathcal{M}_\epsilon T \,\mathrm{d}s = \mathrm{d}(\mu_{\rm g} - \mu_\ell). \tag{55}$$

Using (49) together with results from [8] we obtain the useful pressure differential

$$\tilde{c}^{-2} \,\mathrm{d}p = \mathrm{d}\rho + \rho^2 \Theta \,\mathrm{d}s + \rho^2 \beta \,\mathrm{d}Y. \tag{56}$$

We may now use (56) to recast (55) in terms of the pressure:

$$\beta \,\mathrm{d}p + \nu \,\mathrm{d}Y + \rho T \frac{(s_\ell - s_{\rm g})}{C_{p,{\rm g}} + C_{p,\ell}} \,\mathrm{d}s = \mathrm{d}(\mu_{\rm g} - \mu_\ell). \tag{57}$$

Hence along the saturation line ($\mu_{\rm g} = \mu_\ell$), we may write

$$\left(\frac{\partial Y}{\partial p}\right)_{s,\rm sat} = -\frac{\beta}{\nu} = \frac{1}{\rho^2 \nu} \cdot \left(\frac{\partial \rho}{\partial Y}\right)_{s,p}. \tag{58}$$

From equation (6.15) in [7] we may then write

$$\hat{c}^{-2} = \tilde{c}^{-2} + \beta^2 \frac{\rho^2}{\nu}, \tag{59}$$

and it may now be verified that (42), and hence the subcharacteristic condition in the sense of Definition 1, are satisfied subject only to fundamental thermodynamic stability constraints.

Herein lies the basis for our paper; as we will now see, it is precisely (42) that forms the mathematical mechanism to ensure that the equilibrium mass flux, predicted from energy principles, will locally not exceed the corresponding frozen mass flux.

5. Nozzle flow theory

Having established the energy invariants, we now proceed to describing how these can be used to model flow through chokes and nozzles. Based on Propositions 2, 3, 5 and 6, we make the ideal assumption that the following differential relations are valid throughout such flows.

$$\mathrm{d}s = 0, \tag{60}$$

$$\mathrm{d}\left(h + \tfrac{1}{2}u^2\right) = 0, \tag{61}$$

where h is the mixture enthalpy

$$h = Y h_\mathrm{g} + (1 - Y) h_\ell. \tag{62}$$

We may then state the following proposition.

Proposition 7. For both the frozen and equilibrium models, the following differential relation is valid along streamlines for smooth, steady flows:

$$\mathrm{d}h + u\,\mathrm{d}u = \frac{1}{\rho}\,\mathrm{d}p + (\mu_\mathrm{g} - \mu_\ell)\,\mathrm{d}Y + u\,\mathrm{d}u = 0. \tag{63}$$

Proof. This follows from (38), (60), (61) and (62). □

We now consider flows from some inlet conditions, denoted with the subscript "1", to some outlet conditions denoted with the subscript "o". We assume that the flow is pressure-driven so that

$$p_1 \geq p_\mathrm{o}. \tag{64}$$

5.1. Subcritical flows

Assuming that the flow remains subsonic, the flow will be accelerated until the flow pressure p_2 equilibrates with the outlet pressure, i.e.

$$p_2 = p_o. \tag{65}$$

We also assume that the flow accelerates from stationary conditions, i.e.

$$u_1 = 0. \tag{66}$$

It then follows from (60) and (61) that at the outlet conditions we also have $s_2 = s_1 = s$ as well as

$$u_2^2 = 2\left(h(p_1, Y_1, s) - h(p_o, Y_1, s)\right) \tag{67}$$

for the frozen model and

$$u_2^2 = 2\left(h(p_1, s) - h(p_o, s)\right) \tag{68}$$

for the equilibrium model.

We now assume that the inlet pressure p_1 is fixed but we allow the outlet pressure p_o to vary. We may then obtain a useful relation.

Proposition 8. For the frozen model, characterized by

$$\mathrm{d}Y = 0, \tag{69}$$

as well as for the equilibrium model, characterized by

$$\mu_g = \mu_\ell, \tag{70}$$

the escape velocity u_2 in both cases satisfies

$$\frac{\mathrm{d}u_2}{\mathrm{d}p_o} = -\frac{1}{q_2}, \tag{71}$$

where $q = \rho u$ is the mass flux.

Proof. The result follows directly from using (69) and (70) in (63). □

Note that this implies that the derivative of the velocity diverges in the limit $u \to 0$.

For subcritical flows, a very general result may now be derived.

Proposition 9. Under subcritical conditions, the escape velocities of the two models satisfy the inequality

$$\tilde{u}_2 \leq \hat{u}_2, \tag{72}$$

where $\tilde{u}$ is the velocity of the frozen model and $\hat{u}$ is the velocity in the equilibrium model.

Proof. Integrating (63) along a path of constant mass fraction we obtain

$$\tfrac{1}{2}\tilde{u}_2^2 = h(p_1, Y_1 - h(p_\mathrm{o}, Y_1), \tag{73}$$

whereas integrating along the phase equilibrium curve we obtain

$$\tfrac{1}{2}\hat{u}_2^2 = h(p_1, Y_1) - h\left(p_\mathrm{o}, Y_\mathrm{eq}(p_\mathrm{o})\right), \tag{74}$$

where Y_eq is the phase equilibrium mass fraction. Note that from here onward we neglect the entropy dependence in the notation as s is everywhere constant. We then obtain

$$\tfrac{1}{2}\left(\hat{u}_2^2 - \tilde{u}_2^2\right) = h(p_\mathrm{o}, Y_1) - h(p_\mathrm{o}, Y_\mathrm{eq}) = \int_{Y_\mathrm{eq}}^{Y_1} (\mu_\mathrm{g} - \mu_\ell)\,\mathrm{d}Y \geq 0, \tag{75}$$

where the sign follows from

$$\left(\frac{\partial(\mu_\mathrm{g} - \mu_\ell)}{\partial Y}\right)_{p,s} = \rho T \frac{(s_\ell - s_\mathrm{g})^2}{C_{p,\mathrm{g}} + C_{p,\ell}} \geq 0, \tag{76}$$

which in turn follows from (57). □

We now turn to deriving differentials for the outlet *mass flux* in terms of the outlet pressure. Using

$$\mathrm{d}\rho = \frac{1}{\tilde{c}^2}\,\mathrm{d}p + \left(\frac{\partial \rho}{\partial Y}\right)_p \mathrm{d}Y, \tag{77}$$

we may now write (63) as

$$\mathrm{d}q = \left(\frac{u}{\tilde{c}^2} - \frac{1}{u}\right)\mathrm{d}p + \left(u\left(\frac{\partial \rho}{\partial Y}\right)_p - \frac{\rho}{u}\left(\mu_\mathrm{g} - \mu_\ell\right)\right)\mathrm{d}Y. \tag{78}$$

We now investigate, in turn, the frozen case and the equilibrium case.

- *Frozen model.* In the frozen model, $\mathrm{d}Y = 0$ and we may write (78) as

$$\mathrm{d}q_2 = \left(\frac{\tilde{u}_2}{\tilde{c}_2^2} - \frac{1}{\tilde{u}_2}\right) \mathrm{d}p_\mathrm{o}. \tag{79}$$

- *Equilibrium model.* Now, along the saturation line we have

$$\mathrm{d}Y = \left(\frac{\partial Y}{\partial p}\right)_\mathrm{sat} \mathrm{d}p, \tag{80}$$

so that for paths along this line, we have

$$\mathrm{d}q = \left(\frac{u}{\tilde{c}^2} + u \left(\frac{\partial \rho}{\partial Y}\right)_p \left(\frac{\partial Y}{\partial p}\right)_\mathrm{sat} - \frac{1}{u}\right) \mathrm{d}p. \tag{81}$$

Using (58) and (59), we may write this as

$$\mathrm{d}q_2 = \left(\frac{\hat{u}_2}{\hat{c}_2^2} - \frac{1}{\hat{u}_2}\right) \mathrm{d}p_\mathrm{o}. \tag{82}$$

Proposition 10. If the following equality on the sound velocities holds:

$$\tilde{c}(p, Y_1) > \hat{c}(p) \quad \forall p \in [p_\mathrm{o}, p_1], \tag{83}$$

we have

$$\tilde{q}(p_\mathrm{o}) > \hat{q}(p_\mathrm{o}). \tag{84}$$

Proof. Using (78) and (81), we may write the mass flux difference as

$$\Delta q = \tilde{q} - \hat{q} = \int_{p_\mathrm{o}}^{p_1} \left(\frac{\hat{u}}{\hat{c}^2} - \frac{1}{\hat{u}} - \frac{\tilde{u}}{\tilde{c}^2} + \frac{1}{\tilde{u}}\right) \mathrm{d}p. \tag{85}$$

By Proposition 9 and (83), the integrand and hence the integral are positive. □

Note that (83) is a sufficient, but not necessary, condition for (84) to hold.

We are now in a position to state the main observation of our paper. Assume that the inlet conditions are in phase equilibrium, i.e.

$$Y_1 = Y_\mathrm{eq}(p_1). \tag{86}$$

Then it follows directly from (59), i.e. the *subcharacteristic condition*, that

$$\tilde{c}_1 \geq \hat{c}_1, \tag{87}$$

and in particular, if $\beta \neq 0$ in (59), i.e. the subcharacteristic condition is *strictly satisfied*, then (83) is guaranteed to be satisfied for sufficiently small

$$\Delta p = p_1 - p_{\mathrm{o}}. \tag{88}$$

This is the *direct link* between the general subcharacteristic condition of Chen–Levermore–Liu [6] and the classical nozzle flow theory for mass rates. In particular, we have demonstrated that for this particular relaxation model, the fact that the imposed equilibrium condition will decrease the predicted mass flow rate is a *direct consequence* of the stability condition (42) on the relaxation process.

5.2. Critical flows

From (79) and (82), we recover the well-known fact that the mass flow rate has a critical point at the sonic velocity, i.e.

$$\mathrm{d}q = 0 \qquad \text{when} \qquad u = c. \tag{89}$$

This has a concrete physical interpretation: If $u > c$, then all characteristics would propagate out from the inlet and there would be no way for the flow to receive information about the outlet pressure. Hence, we may define the *critical pressures* $\tilde{p}_{\mathrm{c}}, \hat{p}_{\mathrm{c}}$ implicitly through

$$h(\tilde{p}_{\mathrm{c}}, Y_1) = h(p_1, Y_1) - \tfrac{1}{2}\tilde{c}^2(\tilde{p}_{\mathrm{c}}, Y_1), \tag{90}$$
$$h(\hat{p}_{\mathrm{c}}, Y_{\mathrm{eq}}(\hat{p}_{\mathrm{c}})) = h(p_1, Y_1) - \tfrac{1}{2}\hat{c}^2(\hat{p}_{\mathrm{c}}, Y_{\mathrm{eq}}(\hat{p}_{\mathrm{c}})). \tag{91}$$

These are, according to (73) and (74), precisely the outlet pressures needed to accelerate the flow to the sonic point.

Hence, when taking critical flows into account, the algorithm to calculate the flow rates may be specified as follows:

1. Calculate critical pressures according to (90) and (91).
2. Calculate the outlet pressures according to

$$\tilde{p}_2 = \max(\tilde{p}_{\mathrm{c}}, p_{\mathrm{o}}), \tag{92}$$
$$\hat{p}_2 = \max(\hat{p}_{\mathrm{c}}, p_{\mathrm{o}}). \tag{93}$$

3. Calculate outlet velocities from the constancy of the stagnation enthalpy:

$$\tfrac{1}{2}\tilde{u}_2^2 = h(p_1, Y_1) - h(p_2, Y_1), \tag{94}$$

$$\tfrac{1}{2}\hat{u}_2^2 = h(p_1, Y_1) - h\left(p_2, Y_{\mathrm{eq}}(p_{\mathrm{o}})\right). \tag{95}$$

The remaining thermodynamic variables, e.g. the density, may now be found as functions of the fully determined thermodynamic state (p_2, s).

This defines the complete nozzle flow theory. We now illustrate this by an example, in particular we are interested in evaluating the magnitude of the mass flux difference (85) in the context of Proposition 10.

6. Modeling tank leakage of CO_2

We consider leakage from a tank filled with CO_2 in phase equilibrium. If we assume isentropic leakage, the mass and energy content of the tank will evolve according to the differential equations

$$\frac{\mathrm{d}\rho_1}{\mathrm{d}t} = -Q, \tag{96}$$

$$\frac{\mathrm{d}\rho_1 e_1}{\mathrm{d}t} = -Q h_1, \tag{97}$$

where Q relates to the flow rate q through

$$Q = \frac{A}{V} q_2, \tag{98}$$

where V is the total volume of the tank and A is the cross-sectional area of the tank opening.

We now compare three models for q_2:

1. **FR**: The *frozen* model based on an ideal gas and incompressible liquid;
2. **EQ**: The *equilibrium* model based on an ideal gas and incompressible liquid;
3. **SW EQ**: The *equilibrium* model based on the *Span–Wagner* [27] reference equation-of-state.

6.1. The stiffened gas equation-of-state

The stiffened gas equation-of-state [18, 19] is currently widely used in the CFD community [9, 23] due to its simplicity and flexibility in modeling the thermodynamic properties of liquids, gases and even solids. The stiffened gas model may be fully described by the Helmholtz free energy:

$$A(\rho, T) = c_V T \left(1 - \ln\left(\frac{T}{T_0}\right) + (\gamma - 1)\ln\left(\frac{\rho}{\rho_0}\right)\right) - s_0 T + \frac{p_\infty}{\rho} + e_*. \quad (99)$$

Herein, the parameters c_V, γ, p_∞ and e_* are constants specific to the fluid, and

$$s_0 = s(\rho_0, T_0) \quad (100)$$

defines a reference entropy. From (99) we may now derive all the needed thermodynamic relations, for instance the pressure law

$$p(\rho, e) = (\gamma - 1)\rho(e - e_*) - \gamma p_\infty. \quad (101)$$

We refer to [9] and the references therein for further details. In the following, we will describe how this can be used as a basis for a highly simplified phase transition model by considering the incompressible limit for the liquid and the ideal limit for the gas.

6.1.1. A model for CO_2

We now assume that both the liquid and the gas phase of the mixture are described by a separate equation of state based on (99).

- *Liquid phase.* We consider the incompressible limit of (99), given by

$$A_\ell(T) = c_{V,\ell} T \left(1 - \ln\left(\frac{T}{T_0}\right)\right) + e_{*,\ell} - s_{0,\ell} T, \quad (102)$$

supplemented by

$$\rho_\ell = \text{const.} \quad (103)$$

For our CO_2 model, we use the parameters

$$T_0 = 304.128 \text{ K}, \quad (104)$$

$$e_{*,\ell} = 0, \quad (105)$$

$$s_{0,\ell} = 0, \quad (106)$$

$$\rho_\ell = 1229.25 \text{ kg/m}^3, \quad (107)$$

$$c_{V,\ell} = 2.042 \text{ kJ/(kg} \cdot \text{K)}. \quad (108)$$

- *Gas phase.* We consider the ideal gas limit of (99), given by

$$A_{\mathrm{g}}(\rho, T) = c_{V,\mathrm{g}} T \left(1 - \ln\left(\frac{T}{T_0}\right) + (\gamma - 1)\ln\left(\frac{\rho}{\rho_0}\right)\right) - s_{0,\mathrm{g}} T + e_{*,\mathrm{g}}. \tag{109}$$

For our CO_2 model, we use the parameters

$$\rho_0 = 161.41 \text{ kg/m}^3, \tag{110}$$
$$\gamma = 1.174, \tag{111}$$
$$c_{V,\mathrm{g}} = 863.7 \text{ J/(kg} \cdot \text{K)}, \tag{112}$$
$$e_{*,\mathrm{g}} = 551.616 \text{ kJ/kg}, \tag{113}$$
$$s_{0,\mathrm{g}} = 765.668 \text{ J/(kg} \cdot \text{K)}. \tag{114}$$

Herein, the parameters (104)–(108) and (110)–(114) have been determined by minimizing the global error in density, compared to the Span–Wagner reference equation-of-state [27], in the region defined by

$$p \in [0.528 \text{ MPa}, 7.3773 \text{ MPa}], \tag{115}$$
$$T \in [216.60 \text{ K}, 304.128 \text{ K}]. \tag{116}$$

As usual, phase equilibrium is determined by the chemical potentials being equal, where for our simplified model we may derive:

$$\mu_{\mathrm{g}}(p, T) = \gamma c_{V,\mathrm{g}} \left(1 - \ln\left(\frac{T}{T_0}\right) + \frac{\gamma - 1}{\gamma}\ln\left(\frac{p}{p_0}\right)\right) - s_{0,\mathrm{g}} T + e_{*,\mathrm{g}}, \tag{117}$$
$$\mu_\ell(p, T) = c_{V,\ell}\left(1 - \ln\left(\frac{T}{T_0}\right)\right) + \frac{p}{\rho_\ell}. \tag{118}$$

We now have all the information needed to calculate the flow rate q as described in Section 5.2. Note however, that this involves solving a number of coupled, nonlinear equations. For the simulations presented here, we employed a method based on the Newton–Raphson procedure.

6.2. The Span–Wagner equation-of-state

Having presented a highly simplified model for two-phase mixtures, we now move to the other end of the spectrum. The Span–Wagner [27] equation-of-state is a complex, multi-parameter equation, constructed to model gas-liquid CO_2 to a high degree of accuracy. Within the relevant physical region, the relative error in the density does not exceed 0.05%, and the remaining thermodynamic parameters are also modeled to a similar degree of accuracy.

The degree of complexity of this state equation does however severely limit the usefulness of analytical calculations; for most practical purposes, it must be treated as a black box. However, the Span–Wagner equation is implemented in several available computer codes suitable for interfacing with numerical solvers, for instance the *REFPROP* library [20].

The Span–Wagner equation is formulated in terms of the Helmholtz free energy $A(\rho, T)$ and is therefore in principle able to model mixtures out of phase equilibrium. However, it should be noted that the model is not validated against experimental data in this case. Hence, in the following, only calculations for the equilibrium nozzle flow model will be presented.

6.3. Numerical results

We consider now a tank filled with a CO_2 mixture in phase equilibrium at

$$p_1 = 7 \text{ MPa}, \tag{119}$$

$$T_1 = 300 \text{ K}, \tag{120}$$

containing a leakage of cross-sectional area A connecting the tank to the surroundings at $p_\mathrm{o} = 1$ MPa. In the context of (98), we assume the ratio

$$\frac{A}{V} = 3.60 \cdot 10^{-5} \text{ m}^{-1}, \tag{121}$$

i.e the size of the hole is small compared to the size of the tank.

A fourth-order Runge-Kutta method was used to solve the evolution equations (96)–(97), employing the algorithm described in Section 5.2. The time development of the tank state given by the different models for the nozzle flow is plotted in Figure 1.

We observe the expected result that the EQ model leads to slower drainage from the tank than the FR model. However, note that the SW-EQ model gives quite similar results as the FR model, indicating that the deviation between the frozen and equilibrium model is largely compensated by the deviation between the incompressible liquid/ideal gas and Span–Wagner equations of state.

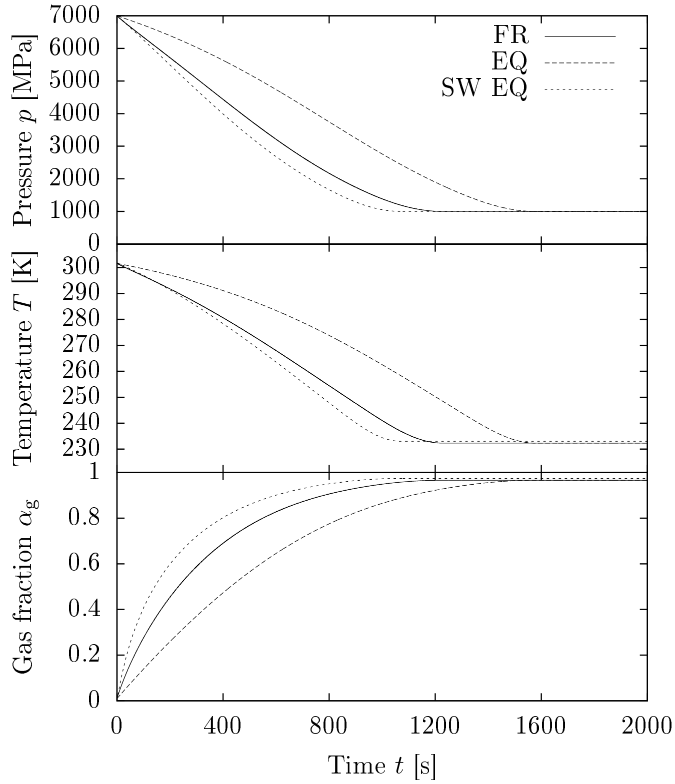

Figure 1: Time development of the tank state.

6.4. Verification of the mass flow principle

The simulation of the previous section illustrates the expected result that the mass flow rate predicted by the frozen model is larger than the corresponding flow rate of the equilibrium model, as stated by the inequality (84). However, as indicated in Section 5.1, this principle can only be guaranteed for sufficiently small

$$\Delta p = p_1 - p_o. \tag{122}$$

We now wish to illustrate the fact that in practice, the principle seems to have a rather large region of validity. We consider again an outlet pressure of

$$p_o = 1 \text{ MPa}, \tag{123}$$

and let the tank state be in phase equilibrium, with mixture variables varying within the region

$$\rho_1 \in [100 \text{ kg/m}^3, 1200 \text{ kg/m}^3], \tag{124}$$

$$(\rho e)_1 \in [1 \cdot 10^8 \text{ kg/(m} \cdot \text{s}^2), 1.1 \cdot 10^9 \text{ kg/(m} \cdot \text{s}^2)]. \tag{125}$$

The difference

$$\Delta q = \tilde{q} - \hat{q} \tag{126}$$

is plotted as a function of the tank state in Figure 2. We observe that the principle (84) is everywhere respected.

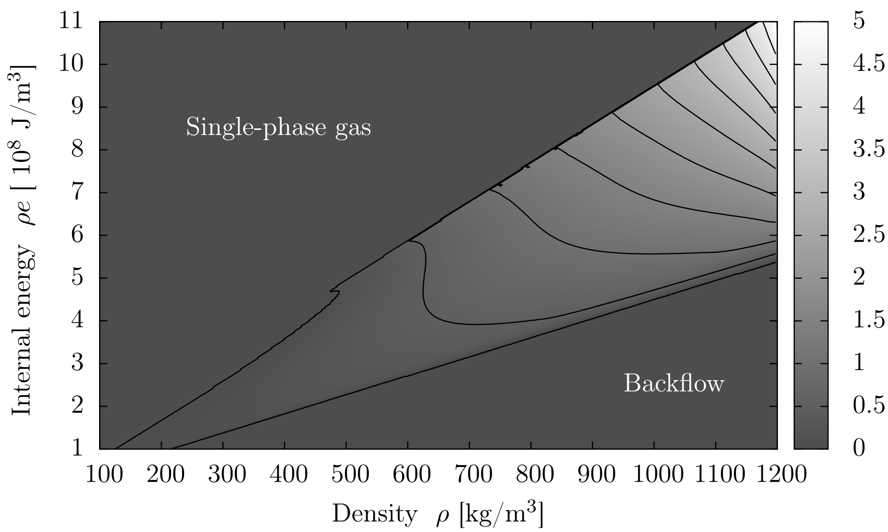

Figure 2: Mass flux difference between frozen and equilibrium models at $p_\text{o} = 1$ MPa, using a CO_2 mixture modeled as an incompressible liquid and ideal gas.

7. Conclusions

We have presented in detail the theory of energy invariants leading up to the *frozen* and *equilibrium* models for the mass rates in two-phase nozzle flow. Herein, some already established results are included for completeness.

The main result of our paper is the observation that the equilibrium flow rate is *guaranteed* to be lower than the frozen flow rate (for sufficiently small pressure differences) as long as

$$\hat{c} \leq \tilde{c}. \tag{127}$$

For this model this is precisely the *subcharacteristic condition* for linear stability, a condition proved to hold for all thermodynamically stable substances.

The relationships (127) and (84) are well-known among fluids engineers. The purpose of this paper has been to put these observations in a more precise theoretical setting. In particular, this direct coupling between the mathematical theory of relaxation systems and nozzle flow, i.e. the relationship between stability and flow rates, has to the best of our knowledge so far never been commented on in the literature.

We have also investigated the magnitude of this effect through a numerical simulation of tank leakage of CO_2. This simulation demonstrated that the difference between the frozen and equilibrium nozzle flow models may be significant; in particular, the difference is similar in magnitude to the error introduced by approximating the thermodynamics with an incompressible liquid/ideal gas assumption.

Acknowledgements

The authors gratefully acknowledge partial financial support from the SINTEF Group. The first author was supported in part by the Research Council of Norway through the BIGCCS centre. The third author was partially supported by the Research Council of Norway through the SIMCOFLOW project.

We are grateful to our colleagues Morten Hammer, Marica Pelanti, Mihaela Popescu and Geir Skaugen for fruitful discussions.

References

[1] K. H. Ardron and R. A. Furness, A study of the critical flow models used in reactor blowdown analysis, *Nucl. Eng. Des.* **39**, 257–266, (1976).

[2] P. Aursand, M. Hammer, S. T. Munkejord and Ø. Wilhelmsen, Pipeline transport of CO_2 mixtures: Models for transient simulation, *Int. J. Greenh. Gas Con.* **15**, 174–185, (2013).

[3] G. Allaire, S. Clerc and S. Kokh, A five-equation model for the simulation of interfaces between compressible fluids, *J. Comput. Phys.* **181**, 577–616, (2002).

[4] R. A. Berry, R. Saurel and O. LeMetayer, The discrete equation method (DEM) for fully compressible, two-phase flows in ducts of spatially varying cross-section. *Nucl. Eng. Des.* **240**, 3797–3818, (2010).

[5] F. Caro, F. Coquel, D. Jamet and S. Kokh, A simple finite-volume method for compressible isothermal two-phase flows simulation, *Int. J. Finite Vol.* **3:(1)**, (2006).

[6] G.-Q. Chen, C. D. Levermore and T.-P. Liu, Hyperbolic conservation laws with stiff relaxation terms and entropy, *Comm. Pure Appl. Math.* **47**, 787–830, (1994).

[7] T. Flåtten and H. Lund, Relaxation two-phase flow models and the subcharacteristic condition, *Math. Models Methods Appl. Sci.* **21**, 2379–2407, (2011).

[8] T. Flåtten, A. Morin and S. T. Munkejord, Wave propagation in multicomponent flow models, *SIAM J. Appl. Math.* **70**, 2861–2882, (2010).

[9] T. Flåtten, A. Morin and S. T. Munkejord, On solutions to equilibrium problems for systems of stiffened gases, *SIAM J. Appl. Math.* **71**, 41–67, (2011).

[10] P. Helluy and N. Seguin, Relaxation models of phase transition flows, *ESAIM: M2AN* **40**, 331–352, (2006).

[11] R. Henry and H. Fauske, The two-phase critical flow of one-component mixtures in nozzles, orifices, and short tubes, *J. Heat Transfer* **93**, 179–187, (1971).

[12] S. Jin and X. Wen, An efficient method for computing hyperbolic systems with geometrical source terms having concentrations, *J. Comput. Math.* **22**, 230–249, (2004).

[13] S. Le Martelot, R. Saurel and O. Le Métayer, Steady one-dimensional nozzle flow solutions of liquid–gas mixtures, *J. Fluid Mech.* **737**, 146–175, (2013)

[14] J. Leray, *Hyperbolic Differential Equations*, The Institute for Advanced Study, (1953).

[15] T.-P. Liu, Hyperbolic conservation laws with relaxation, *Commun. Math. Phys.*, **108**, 153–175, (1987).

[16] H. Lund, A hierarchy of relaxation models for two-phase flow, *SIAM J. Appl. Math.* **72**, 1713–1741, (2012).

[17] H. Mahgerefteh, S. Brown and S. Martynov, A study of the effects of friction, heat transfer, and stream impurities on the decompression behavior in CO_2 pipelines, *Greenhouse Gas. Sci. Technol.* **2**, 369–379, (2012).

[18] R. Menikoff, *Empirical EOS for solids*, in Shock Wave Science and Technology Reference Library, Volume 2 – Solids, Springer-Verlag, Berlin, 143-188, (2007).

[19] R. Menikoff and B. J. Plohr, The Riemann problem for fluid flow of real materials, *Rev. Modern Phys.* **88**, 75-130, (1989).

[20] `http://www.nist.gov/`

[21] H. O. Nordhagen, S. Kragset, T. Berstad, A. Morin, C. Dørum and S. T. Munkejord, A new coupled fluid-structure modelling methodology for running ductile fracture, *Computers & Structures* **94–95**, 13–21, (2012).

[22] A. Oke, H. Mahgerefteh, I. Economou and Y. Rykov, A transient outflow model for pipeline puncture, *Chem. Eng. Sci.* **58**, 4591–4604, (2003).

[23] M. Pelanti and K.-M. Shyue, A mixture-energy-consistent six-equation two-phase numerical model for fluids with interfaces, cavitation and evaporation waves, *J. Comput. Phys.* **259**, 331–357, (2014).

[24] G. A. Reigstad, Numerical network models and entropy principles for isothermal junction flow, *Netw. Heterog. Media* **9**, 65–95, (2014).

[25] S. Solem, P. Aursand and T. Flåtten, The dispersive wave dynamics of a two-phase flow relaxation model, *ESAIM: M2AN*, in press.

[26] S. Solem, P. Aursand and T. Flåtten, Wave dynamics of linear hyperbolic relaxation systems, *J. Hyberbol. Differ. Eq.*, to appear.

[27] R. Span and W. Wagner, A new equation of state for carbon dioxide covering the fluid region from the triple-point temperature to 1100 K at pressures up to 800 MPa, *J. Phys. Chem. Ref. Data* **25**, 1509–1596, (1996).

[28] G. P. Sutton and O. Biblarz, *Rocket propulsion elements,* John Wiley & Sons, New York, (2011).

[29] G. B. Wallis, Critical two-phase flow, *Int. J. Multiphase Flow* **6**, 97–112, (1980).

[30] G. B. Whitham, *Linear and Nonlinear Waves,* John Wiley & Sons, New York, (1974).

[31] W.-A. Yong, Basic aspects of hyperbolic relaxation systems, in Advances in the Theory of Shock Waves, *Progr. Nonlinear Differential Equations Appl.* **47**, 259–305, Birkhäuser Boston, Boston, (2001).